

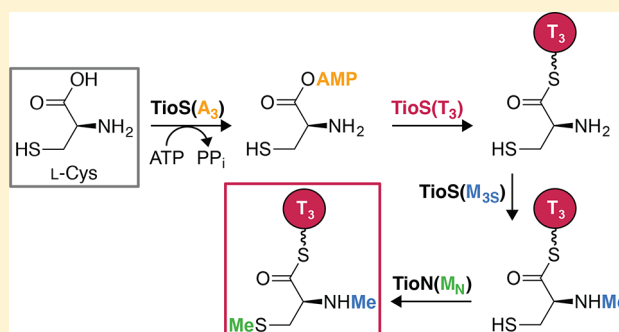
Deciphering Nature's Intricate Way of *N,S*-Dimethylating L-Cysteine: Sequential Action of Two Bifunctional Adenylation Domains

Shogo Mori, Atefeh Garzan, Oleg V. Tsodikov, and Sylvie Garneau-Tsodikova*¹

Department of Pharmaceutical Sciences, College of Pharmacy, University of Kentucky, Lexington, Kentucky 40536-0596, United States

S Supporting Information

ABSTRACT: Dimethylation of amino acids consists of an interesting and puzzling series of events that could be achieved, during nonribosomal peptide biosynthesis, either by a single adenylation (A) domain interrupted by a methyltransferase (M) domain or by the sequential action of two of such independent enzymes. Herein, to establish the method by which Nature *N,S*-dimethylates L-Cys, we studied its formation during thiochondriline A biosynthesis by evaluating TioS(A_{3a}M_{3S}A_{3b}T₃) and TioN(A_aM_NA_b). This study not only led to identification of the exact pathway followed in Nature by these two enzymes for *N,S*-dimethylation of L-Cys, but also revealed that a single interrupted A domain can *N,N*-dimethylate amino acids, a novel phenomenon in the nonribosomal peptide field. These findings offer important and useful insights for the development and engineering of novel interrupted A domain enzymes to serve, in the future, as tools for combinatorial biosynthesis.



Natural products have been and continue to be a very important source of drugs and drug leads.¹ Members of one of the largest families of natural products, the non-ribosomal peptides (NRPs), are biosynthesized on mega-enzymes termed nonribosomal peptide synthetases (NRPSs).² NRPSs are separated into modules that work sequentially to assemble amino acid-like building blocks into short peptides, which are usually further modified to form complex natural products. Each basic NRPS module consists of three core domains: an adenylation (A), a thiolation (T), and a condensation (C) domain. The role of the A domain is to activate its specifically selected substrate to its AMP counterpart by using adenosine triphosphate (ATP). Once adenylated, the substrate is transferred onto the thiol group of the phosphopantetheine (Ppant) arm of its holo (active) T domain partner, which is generated by posttranslational modification of the apo (inactive) enzyme by a phosphopantetheinyltransferase (PPTase) and coenzyme A (CoA). Finally, a C domain catalyzes condensation of the substrates tethered to its surrounding T domains to form an amide bond. This sequence of events is repeated in a successive manner, working from the most upstream to the most downstream module of the NRPS assembly-line, to eventually produce an NRP chain. This NRP chain can be modified during its assembly by auxiliary domains incorporated into NRPS modules, such as methyltransferase (M), oxidase (Ox), epimerase (E), cyclizase (Cy), halogenase (Hal), and ketoreductase (KR) domains.³ These auxiliary domains, with M being one of the most common, are major sources of diversification of NRPs.⁴

As methylation is an important and prevalent modification of natural products, it has attracted a great deal of attention in the

natural product community. Because methylation may beneficially alter the activity of natural products,⁵ engineered methyltransferases⁶ or ones (naturally occurring or engineered) with promiscuous activity^{7–10} have been investigated as biocatalysts for the synthesis of novel bioactive compounds. However, although very important, M domains, which are commonly found embedded in A domains of NRPSs, remain poorly understood.¹¹ So far, all that is known about these M domains embedded into A domains is that (i) the resulting A_aMA_b enzymes are bifunctional,^{12,13} (ii) they can be engineered (by removal or swapping of M domains),¹⁴ and (iii) in some cases, methylation occurs after adenylation.¹³ It has also been noted that auxiliary domains can be inserted into various areas of A domains,¹¹ which comprise 10 conserved core signature sequence motifs (a1–a10).¹⁵ The majority of interrupted A domains have their M domains embedded between their a8 and a9 motifs.^{16,17} So far, only one example of an M domain placed within the relatively long amino acid sequence between the a2 and a3 motifs of an A domain, TioN(A_aM_NA_b), has been found in natural product gene clusters. We previously preliminarily demonstrated that TioN(A_aM_NA_b) is capable of adenylating and methylating L-Cys without confirming the exact methylated product (*N*-Me-L-Cys, *S*-Me-L-Cys, or *N,S*-diMe-L-Cys) that it generated.¹³

Some of the major questions that remain unanswered about these bifunctional enzymes are (i) whether methylation occurs

Received: September 29, 2017

Revised: October 21, 2017

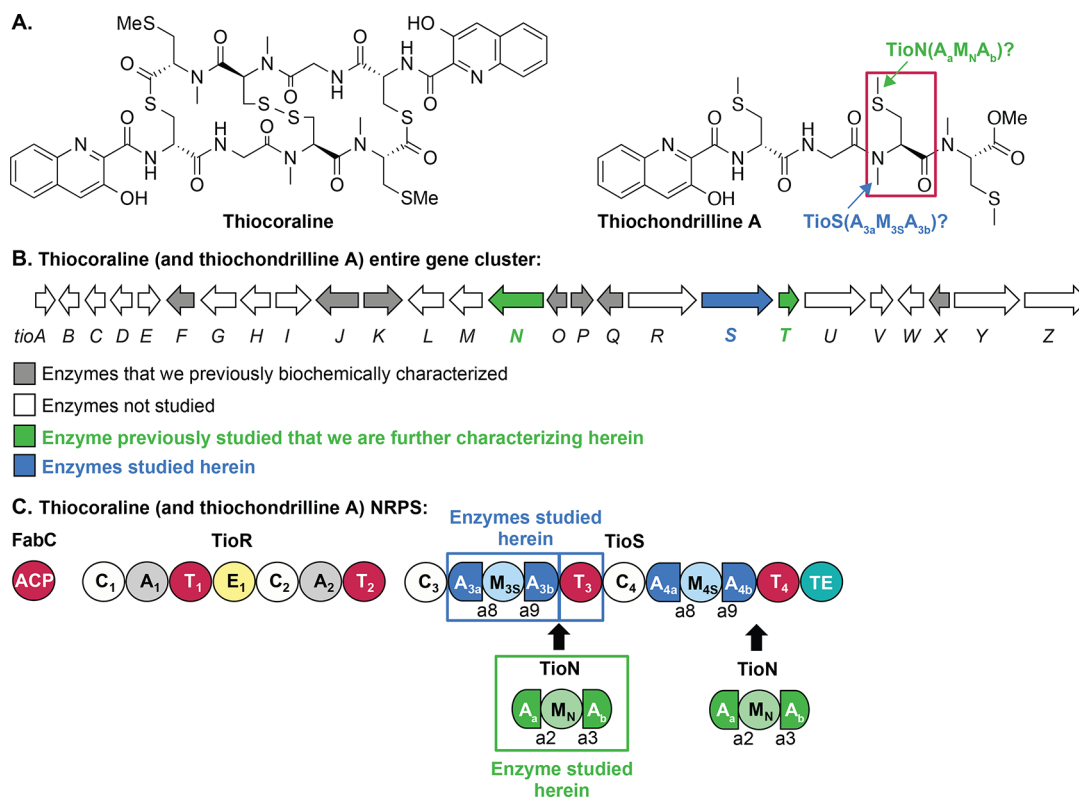


Figure 1. (A) Structures of thiocoraline and thiochondrilline A (a metabolite from *Verrucosipora* sp. isolated from the sponge *Chondrilla caribensis* f. *caribensis*). (B) Thiocoraline (and thiochondrilline A) gene cluster from which both NRPs are biosynthesized. (C) Structural organization of the thiocoraline (and thiochondrilline A) NRPS. Abbreviations: A, adenylation; ACP, acyl carrier protein; C, condensation; T, thiolation; E, epimerization; M, methylation; TE, thioesterase.

(a) pre- or post-adenylation or (b) pre- or post-thiolation, (ii) (a) whether two interrupted A domains sequentially methylate the backbone and side chain (or vice versa) of an amino acid to dimethylate it and, if so, (b) the order in which the backbone versus side-chain methylations occur, and (iii) whether one interrupted A domain can perform both backbone and side-chain methylation on a given amino acid residue.

As our group has a long-standing interest in understanding the unique transformations involved in thiocoraline and thiochondrilline A biosyntheses,^{18–23} as well as in adenylation domains^{24,25} and methyltransferase enzymes,^{12,13,26} to answer these questions, we found the *N,S*-diMe-*L*-Cys residue of thiocoraline²⁷ and thiochondrilline A²⁸ to be a highly suitable model (Figure 1A). By comparing the structures of thiocoraline and thiochondrilline A and by examining their common gene cluster and NRPS assembly-line (Figure 1B,C), we postulated that $\text{TioS}(\text{A}_{3a}\text{M}_{3S}\text{A}_{3b}\text{T}_3)$, a part of the TioS protein ($\text{C}_3\text{-A}_{3a}\text{M}_{3S}\text{A}_{3b}\text{-T}_3\text{-C}_4\text{-A}_{4a}\text{M}_{4S}\text{A}_{4b}\text{-T}_4\text{-TE}$), and the stand-alone $\text{TioN}(\text{A}_2\text{M}_N\text{A}_2)$ could be responsible for backbone and side-chain methylation of *L*-Cys, respectively, during the formation of one of the *N,S*-diMe-*L*-Cys residues (Figure 1A, highlighted by a red box) found in the thiochondrilline A structure. On the basis of this hypothesis, the *N,S*-diMe-*L*-Cys covalently tethered to $\text{TioS}(\text{T}_3)$ [*N,S*-diMe-*L*-Cys-S- $\text{TioS}(\text{T}_3)$] could be produced via one of 12 potential unique pathways (Figure 2, pathways $a_1\text{--}a_4$ to $l_1\text{--}l_4$). Herein, by deciphering Nature's clever and intricate way of *N,S*-dimethylating *L*-Cys, we answer the major remaining questions posed above about bifunctional adenylation/methylating enzymes.

MATERIALS AND METHODS

Bacterial Strains, Plasmids, Materials, and Instrumentation. The $\text{TioN}(\text{A}_2\text{M}_N\text{A}_2)$ ¹³ and Sfp^{29} proteins were overexpressed and purified using previously described procedures. Chemically competent *Escherichia coli* TOP10 cells were purchased from Invitrogen (Carlsbad, CA). The *E. coli* BL21 (DE3)ybdZ::aac(3)IV strain used for co-expression of $\text{TioS}(\text{A}_{3a}\text{M}_{3S}\text{A}_{3b})$ with TioT was a generous gift from M. G. Thomas (University of Wisconsin—Madison, Madison, WI). The pET28a and pACYCDuet-1 overexpression vectors were bought from Novagen (Gibbstown, NJ). DNA primers for polymerase chain reaction (PCR) were purchased from Sigma-Aldrich (St. Louis, MO). Restriction enzymes, Phusion DNA polymerase, T4 DNA ligase, and all other cloning reagents were purchased from New England BioLabs (Ipswich, MA). All chemicals (with the exception of those presented below) and buffer components were purchased from Sigma-Aldrich or VWR and used without any further purification. All reagents for chemical syntheses were purchased from commercial sources and used without any further purification. ¹H nuclear magnetic resonance (NMR) spectra were recorded on a 400 MHz NMR spectrometer (Varian Inova) using CDCl₃ or D₂O. Chemical shifts (δ) are referenced to residual solvent peaks and are reported in parts per million. All reactions were performed under a nitrogen atmosphere, and all reported yields represent isolated yields. All compounds were characterized by ¹H NMR and were in complete agreement with characterizations reported in the literature for these compounds. All compounds are $\geq 95\%$ pure according to NMR spectra. [*methyl*-³H]SAM (*S*-adenosyl-*L*-methionine), [³H]AcCoA, [³²P]PP_i, and [³⁵S]-*L*-

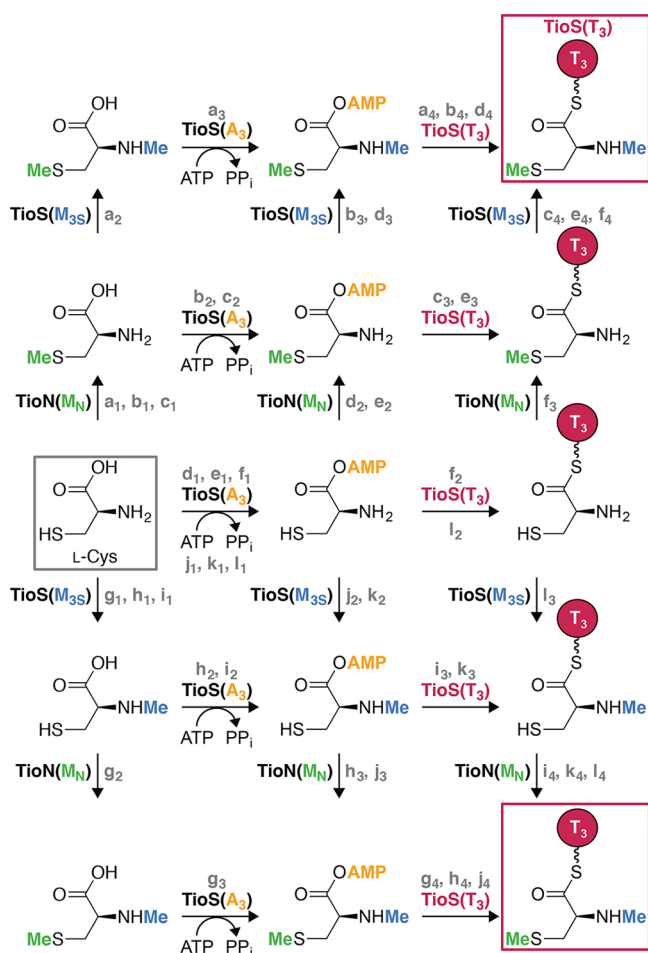


Figure 2. Twelve potential pathways (a–l, with four steps each) for the formation of *N,S*-dimethyl-*L*-Cys-*S*-TioS(T_3) by TioN($A_3M_NA_b$) and TioS($A_{3a}M_{3S}A_{3b}$).

Cys were purchased from PerkinElmer (Waltham, MA). EcoLume liquid scintillation cocktail was purchased from MP biomedical (Santa Ana, CA). Radioactivity was counted by using a TriCarb 2900TR liquid scintillation analyzer (PerkinElmer). DNA sequencing was performed at Eurofins Scientific (Louisville, KY).

Chemical Synthesis and Characterization of Compounds To Be Used as Potential Substrates. *Synthesis of *N*-Methyl-*L*-cysteine Hydrochloride.* The known *N*-methyl-*L*-cysteine hydrochloride was prepared as follows. Boc-Cys(Trt)-OH (0.50 g, 1.08 mmol) was dissolved in tetrahydrofuran (THF) (1 mL) and the mixture added to a solution of NaH (0.10 g, 2.59 mmol, 60% suspension in mineral oil) in THF (3.5 mL) at 0 °C dropwise. MeI (0.22 mL, 3.56 mmol) was added, and the reaction mixture was stirred at room temperature for 12 h. MeOH and H₂O were then added to quench the reaction mixture, which was then acidified with HCl (1 N) to pH ~5. The reaction mixture was extracted with EtOAc, and the organic layer was concentrated under reduced pressure. The residue was dissolved in CH₂Cl₂ (2 mL) followed by addition of triisopropylsilane (1.11 mL, 5.40 mmol) and TFA (2.15 mL, 28.08 mmol). The reaction mixture was stirred at room temperature for 2 h. The reaction mixture was evaporated and treated with H₂O (3 mL) and extracted with Et₂O (3 × 3 mL). The reaction mixture was evaporated to dryness under reduced pressure to give a residue, which was

acidified with HCl (1 N). The reaction mixture was evaporated to dryness under reduced pressure to afford *N*-methyl-*L*-cysteine hydrochloride (0.14 g, 74%) as a light yellow solid: ¹H NMR (400 MHz, D₂O, which matches the literature³⁰) δ 4.18 (t, *J* = 4.4 Hz, 1H), 3.24 (dd, *J* = 15.6, 4.4 Hz, 1H), 3.11 (dd, *J* = 15.6, 4.4 Hz, 1H), 2.76 (s, 3H).

*Synthesis of *N*-Boc-*S*-methyl-*L*-cysteine.* The known *N*-Boc-*S*-methyl-*L*-cysteine was prepared as follows. (Boc)₂O (0.89 g, 4.07 mmol) was added to a solution of *S*-methyl-*L*-cysteine (0.50 g, 3.70 mmol) and NaHCO₃ (0.78 g, 9.25 mmol) in 1,4-dioxane (10 mL) and H₂O (15 mL). The reaction mixture was stirred at room temperature for 12 h. The reaction mixture was treated with H₂O (10 mL) and acidified with HCl (1 N) to pH ~3. The reaction mixture was extracted with EtOAc (3 × 10 mL), and the organic layer was concentrated under reduced pressure to afford *N*-Boc-*S*-methyl-*L*-cysteine (0.87 g, 100%) as a colorless oil: ¹H NMR (400 MHz, CDCl₃, which matches the literature³¹) δ 5.37 (m, 1H), 4.52 (m, 1H), 2.96 (m, 2H), 2.13 (s, 3H), 1.43 (s, 9H).

*Synthesis of *N,S*-Dimethyl-*L*-cysteine Hydrochloride.* The known *N,S*-dimethyl-*L*-cysteine hydrochloride was prepared as follows. *N*-Boc-*S*-methyl-*L*-cysteine (0.587 g, 3.70 mmol) was dissolved in THF (3 mL) and the mixture added to a solution of NaH (0.36 g, 8.88 mmol, 60% suspension in mineral oil) in THF (12 mL) at 0 °C dropwise. MeI (0.76 mL, 12.21 mmol) was added, and the reaction mixture was stirred at room temperature for 12 h. MeOH and H₂O were then added to quench the reaction, and the mixture was then acidified with HCl (1 N) to pH ~5. The reaction mixture was extracted with EtOAc, and the organic layer was concentrated under reduced pressure. The residue was dissolved in HCl (3 mL, 3 N solution in EtOAc). The reaction mixture was stirred at room temperature for 2 h. The reaction mixture was treated with H₂O (3 mL) and washed with EtOAc (3 × 3 mL). The reaction mixture was evaporated to dryness under reduced pressure to afford *N,S*-dimethyl-*L*-cysteine hydrochloride (0.27 g, 60%) as a yellow wax: ¹H NMR (400 MHz, D₂O, which matches the literature³⁰) δ 4.19 (td, *J* = 5.6, 1.2 Hz, 1H), 3.19 (d, *J* = 5.6 Hz, 2H), 2.79 (s, 3H), 2.58 (br s, 1H), 2.16 (s, 3H).

Synthesis of 2-Ethylacrylic Acid. To a mixture of 2-ethylmalonic acid (1.00 g, 7.57 mmol) and diethylamine (2.34 mL, 22.71 mmol) in EtOAc (10 mL) was added paraformaldehyde (0.34 g, 11.36 mmol) at 0 °C. The resulting mixture was refluxed for 12 h. The reaction mixture was treated with H₂O (10 mL) and acidified with HCl (1 N) to pH ~1. The reaction mixture was extracted with EtOAc (3 × 10 mL), and the organic layer was concentrated under reduced pressure to afford the known 2-ethylacrylic acid (0.49 g, 64%) as a light yellow oil: ¹H NMR (400 MHz, CDCl₃, which matches the literature³²) δ 6.27 (s, 1H), 5.64 (d, *J* = 1.6 Hz, 1H), 2.31 (q, *J* = 7.6 Hz, 2H), 1.09 (t, *J* = 7.6 Hz, 3H).

Synthesis of 2-Acetylsulfanylmethylbutyric Acid. A mixture of 2-ethylacrylic acid (0.27 g, 2.70 mmol) and thioacetic acid (0.73 mL, 10.26 mmol) in benzene (5 mL) was refluxed for 12 h. The solution was concentrated under reduced pressure, diluted with EtOAc, and washed with HCl (1 N). The organic layer was concentrated under reduced pressure to afford the known 2-acetylsulfanylmethylbutyric acid (0.40 g, 83%) as a yellow oil: ¹H NMR (400 MHz, CDCl₃, which matches the literature³²) δ 3.11 (dd, *J* = 13.6, 5.6 Hz, 1H), 3.01 (dd, *J* = 13.6, 8.8 Hz, 1H), 2.55 (p, *J* = 7.6 Hz, 1H), 2.31 (s, 3H), 1.73–1.62 (m, 2H), 0.97 (t, *J* = 7.6 Hz, 3H).

Synthesis of 2-Mercaptomethylbutyric Acid (MMB). 2-Acetylsulfanylmethylbutyric acid (0.20 g, 1.13 mmol) was dissolved in HCl (4 mL, 6 N solution in H₂O). The resulting mixture was refluxed for 12 h. The reaction mixture was extracted with EtOAc (3 × 5 mL), and the organic layer was concentrated under reduced pressure to afford the known 2-mercaptomethylbutyric acid (0.12 g, 80%) as a colorless oil: ¹H NMR (400 MHz, CDCl₃, which matches the literature³²) δ 2.82–2.74 (m, 1H), 2.69–2.62 (m, 1H), 2.53 (p, J = 7.6 Hz, 1H), 1.77–1.63 (m, 2H), 1.52 (t, J = 8.8 Hz, 1H), 0.96 (t, J = 7.6 Hz, 3H).

Synthesis of 3-Mercaptopyruvic Acid (MP). Thioacetic acid (0.32 mL, 4.49 mmol) was added to a mixture of bromopyruvic acid (0.50 g, 2.99 mmol) in THF (9 mL) at 0 °C dropwise. Et₃N (0.50 mL, 3.59 mmol) was added, and the reaction mixture was stirred at room temperature for 12 h. H₂O was then added to quench the reaction, and the mixture was then acidified with HCl (1 N) to pH ~1. The reaction mixture was extracted with EtOAc, and the organic layer was concentrated under reduced pressure. The residue was dissolved in HCl (11 mL, 6 N solution in H₂O). The reaction mixture was refluxed for 12 h. The reaction mixture was treated with H₂O (10 mL) at room temperature and extracted with EtOAc (3 × 10 mL). The reaction mixture was evaporated to dryness under reduced pressure to afford the known 3-mercaptopyruvic acid (0.25 g, 69%) as a yellow oil: ¹H NMR (400 MHz, CDCl₃, which matches the literature³³) δ 4.41 (s, 2H), 4.17 (br s, 1H).

Preparation of pTioS(A_{3a}M₃₅A_{3b})-pET28a and pTioS-(T₃)-pET28a Overexpression Constructs. The truncated *tioS* genes, *tioS*(A_{3a}M₃₅A_{3b}) and *tioS*(T₃), were amplified from genomic DNA of *Micromonospora* sp. ML1 by PCR with the forward and reverse primers *tioS*(A_{3a}M₃₅A_{3b})-*fwd* and *tioS*(A_{3a}M₃₅A_{3b})-*rev*, respectively, for *tioS*(A_{3a}M₃₅A_{3b}) or *tioS*(T₃)-*fwd* and *tioS*(T₃)-*rev*, respectively, for *tioS*(T₃) (Table S1). PCRs were performed in reaction mixtures consisting of 0.25 μL of Phusion High-Fidelity DNA polymerase, 5 μL of Phusion GC Buffer, 15 ng of *Micromonospora* sp. ML1 genomic DNA, 0.25 μL each of 50 μM forward and reverse primer, 0.5 μL of 10 mM dNTP, 1.5 μL of DMSO, and 16.25 μL of ddH₂O for a total volume of 25 μL. The PCR conditions were optimized as follows: initial denaturation for 30 s at 98 °C, 30 cycles of 30 s at 98 °C, 30 s at 72 °C, and 3.5 min for *tioS*(A_{3a}M₃₅A_{3b}) or 1.5 min for *tioS*(T₃) at 72 °C, and a final extension for 10 min at 72 °C. The DNA fragments of *tioS*(A_{3a}M₃₅A_{3b}) and *tioS*(T₃) were purified by agarose gel extraction using the QIAquick Gel Extraction Kit (Qiagen, Valencia, CA), and they were digested by restriction enzymes *Nde*I and *Hind*III. After being purified by agarose gel extraction again, the DNA fragments were ligated between the *Nde*I and *Hind*III multiple cloning sites of expression plasmid vector pET28a (Novagen), which contains a His₆ tag at the 5'-end. The resulting plasmids pTioS-(A_{3a}M₃₅A_{3b})-pET28a and pTioS-(T₃)-pET28a were transformed into a chemically competent *E. coli* TOP10 strain and cultured on Luria-Bertani (LB) agar supplemented with 50 μg/mL kanamycin overnight. A colony of each construct was subsequently cultured in 5 mL of LB medium with the antibiotic overnight for plasmid isolation by the QIAprep Spin Miniprep Kit (Qiagen). Successful cloning of the genes was confirmed by sequencing reactions of the purified plasmids, which match the sequence of UniProtKB entry Q333U7 for *tioS*(A_{3a}M₃₅A_{3b}) and *tioS*(T₃).

Co-Overexpression and Purification of TioS-(A_{3a}M₃₅A_{3b}) with TioT. TioS(A_{3a}M₃₅A_{3b}) was overexpressed

with its MbtH-like protein partner TioT for which the cloning was previously reported.²⁰ pTioS(A_{3a}M₃₅A_{3b})-pET28a was transformed into chemically competent *E. coli* strain BL21 (DE3)ybdZ::aac(3)IV in which pTioT-pACYCDuet-1 was previously transformed. This was cultured on LB agar supplemented with 50 μg/mL kanamycin and 35 μg/mL chloramphenicol. The protein was overexpressed in 3 × 1 L of LB medium supplemented with 50 μg/mL kanamycin, 35 μg/mL chloramphenicol, and 10 mM MgCl₂. The transformant was incubated in 3 × 5 mL of LB medium with the antibiotics overnight. Each 5 mL culture was inoculated into 1 L of LB medium with the antibiotics and MgCl₂ (10 mM) and grown at 37 °C and 200 rpm until the OD₆₀₀ reached 0.6–0.8. Protein expression was then induced with 0.2 mM isopropyl β-D-1-thiogalactopyranoside (IPTG), and the bacterial culture was incubated at 16 °C and 200 rpm for 20 h. The cells were harvested by centrifugation at 5000 rpm for 10 min at 4 °C. They were subsequently washed with H₂O and buffer A [25 mM Tris-HCl, 400 mM NaCl, and 10% glycerol (pH 8.0)] supplemented with 5 mM imidazole followed by resuspension in 30 mL of buffer A supplemented with 5 mM imidazole, 1 mM dithiothreitol (DTT), and 1 mM phenylmethanesulfonyl fluoride (PMSF). This was lysed by sonication (four cycles of 2 min alternating with 2 s “on” and 10 s “off”), and the cell debris was removed by centrifugation at 16000 rpm for 45 min at 4 °C. The supernatant was incubated with 0.75 mL of washed Ni^{II}-NTA agarose resin (Qiagen) at 4 °C for 2 h while being gently shaken. The resin was loaded onto a column and washed with 10 × 10 mL of buffer A supplemented with 40 mM imidazole, and TioS(A_{3a}M₃₅A_{3b}) and TioT were co-eluted with 3 × 5 mL of buffer A supplemented with 500 mM imidazole. After sodium dodecyl sulfate–polyacrylamide gel electrophoresis (SDS–PAGE) analysis, the first two elution fractions that contained the protein of interest were dialyzed in 3 × 2 L of buffer B [40 mM Tris-HCl, 200 mM NaCl, 2 mM β-mercaptoethanol, and 10% glycerol (pH 8.0)] at 4 °C for a total of 20 h. The resulting solution was concentrated by using Amicon Ultra-15 Centrifugal Filter Units (EMD Millipore, Billerica, MA) with a 3 kDa molecular weight cutoff (MWCO) membrane, and the protein concentration was spectrophotometrically determined by using the calculated extinction coefficient at 280 nm (<http://protecalc.sourceforge.net/cgi-bin/protecalc>). The yield of TioS(A_{3a}M₃₅A_{3b}) with TioT was 1.34 mg/L of culture (Figure S2).

Substrate Specificity and Determination of Kinetic Parameters of the A Domains of TioS(A_{3a}M₃₅A_{3b}) and TioN(A_aM_NA_b) by ATP-[³²P]PP_i Exchange Assays. To evaluate the substrate specificity and kinetics of the A domains of TioS(A_{3a}M₃₅A_{3b}) and TioN(A_aM_NA_b), ATP-[³²P]PP_i exchange assays were performed. For the substrate profiles, each 100 μL reaction {75 mM Tris-HCl, 5 mM TCEP, 10 mM MgCl₂, 5 mM ATP, 1 mM Na₄P₂O₇ with ~400000 cpm of [³²P]PP_i, 5 mM substrate [L-Cys, N-Me-L-Cys, S-Me-L-Cys, N,S-diMe-L-Cys, L-Ser, L-Thr, L-Ala, L-Gly, L-Val, L-Leu, L-Ile, L-Pro, L-Phe, L-Tyr, L-Trp, L-Met, L-Asn, L-Gln, L-Lys, L-Arg, L-His, L-Asp, L-Glu, 2-mercaptomethylbutyric acid (MMB), or 3-mercaptopyruvic acid (MP)], and 1.0 μM TioS(A_{3a}M₃₅A_{3b}) or 2.5 μM TioN(A_aM_NA_b), at pH 7.5} was initiated by adding the substrate and each mixture incubated for 2 h at room temperature. The reactions were quenched by adding 500 μL of the quenching solution [1.6% (w/v) activated charcoal, 4.5% (w/v) Na₄P₂O₇, and 3.5% (v/v) perchloric acid in H₂O]. The charcoal was pelleted by centrifugation for 7 min at 14000 rpm

Table 1. Steady-State Kinetic Parameters for AMP Derivatization by TioS(A_{3a}M_{3s}A_{3b}) or TioN(A_aM_NA_b)

protein	substrate	K _m (mM)	k _{cat} (min ⁻¹)	k _{cat} /K _m (mM ⁻¹ min ⁻¹)
TioS(A _{3a} M _{3s} A _{3b})	L-Cys	0.140 ± 0.003	7.72 ± 0.03	55.4 ± 1.4
	N-Me-L-Cys	2.2 ± 0.2	8.7 ± 0.3	4.0 ± 0.4
	S-Me-L-Cys	10.0 ± 0.7	6.5 ± 0.2	0.66 ± 0.05
TioN(A _a M _N A _b)	L-Cys	0.037 ± 0.001	4.13 ± 0.02	111 ± 4
	N-Me-L-Cys	1.1 ± 0.2	5.3 ± 0.3	5.0 ± 0.9
	S-Me-L-Cys	3.5 ± 0.1	3.72 ± 0.05	1.06 ± 0.04

and washed twice with 500 μL of the wash solution [4.5% (w/v) Na₄P₂O₇ and 3.5% (v/v) perchloric acid in H₂O]. Each of these was subsequently resuspended in 500 μL of H₂O and added to a scintillation vial containing 5 mL of scintillation cocktail, whose radioactivity was counted by the liquid scintillation analyzer. The substrate profiles are presented in Figure 3.

The kinetic parameters of TioS(A_{3a}M_{3s}A_{3b}) and TioN(A_aM_NA_b) were calculated by the reaction rate with each substrate (L-Cys, N-Me-L-Cys, and S-Me-L-Cys). The 100 μL reactions [75 mM Tris-HCl, 5 mM TCEP, 10 mM MgCl₂, 5 mM ATP, 1 mM Na₄P₂O₇ with ~400000 cpm of [³²P]PP_i, varied concentrations of substrate (0, 0.05, 0.1, 0.25, 0.5, 1, 1.75, 2.5, 5, 10, and ≤15 mM until the substrate starts inhibiting the reaction), and 1.0 μM TioS(A_{3a}M_{3s}A_{3b}) or 2.5 μM TioN(A_aM_NA_b), at pH 7.5] were initiated by adding the substrate and the mixtures incubated at room temperature for 12 min for TioS(A_{3a}M_{3s}A_{3b}) and 15 min for TioN(A_aM_NA_b), where the adenylation rate is in a linear range. The reaction mixtures were processed and counted by the same method as that described for the substrate profile assay. Because the kinetic parameters of TioN(A_aM_NA_b) with N,S-diMe-L-Cys could not be determined because of enzyme inhibition by high concentration of the substrate, the activity was measured in a time course assay (Figure S5). Each 100 μL reaction [75 mM Tris-HCl, 5 mM TCEP, 10 mM MgCl₂, 5 mM ATP, 1 mM Na₄P₂O₇ with ~400000 cpm of [³²P]PP_i, 5 mM substrate, and 2.5 μM TioN(A_aM_NA_b), at pH 7.5] was initiated by adding the substrate and each mixture incubated for 0, 0.5, 1, 2, 4, 8, and 12 h at room temperature. The reactions were quenched and the mixtures processed by the same method as that described for the substrate profile assay. All experiments were performed in at least duplicate. The steady-state kinetic parameters are listed in Table 1 and presented in Figures S3 and S4.

Overexpression and Purification of TioS(T₃). pTioS-(T₃)-pET28a was transformed into chemically competent *E. coli* BL21 (DE3), which was cultured on LB agar supplemented with 50 μg/mL kanamycin. The transformant was incubated in 3 × 5 mL of LB medium with the antibiotic overnight. Each 5 mL culture was inoculated into 1 L of LB with the antibiotic and grown at 37 °C and 200 rpm until the OD₆₀₀ reached 0.6–0.8. Protein expression was then induced with 0.2 mM IPTG, and the bacterial culture was incubated at 16 °C and 200 rpm for 20 h. The cells were harvested by centrifugation at 5000 rpm for 10 min at 4 °C. They were subsequently washed with H₂O and buffer A supplemented with 5 mM imidazole followed by resuspension in 30 mL of buffer A supplemented with 5 mM imidazole, 1 mM DTT, and 1 mM PMSF. This was lysed by sonication (four cycles of 2 min alternating with 2 s “on” and 10 s “off”), and the cell debris was removed by centrifugation at 16000 rpm for 45 min at 4 °C. The supernatant was incubated with 0.75 mL of washed Ni^{II}-NTA agarose resin (Qiagen) at 4 °C for 2 h while being gently shaken. The resin was loaded

onto a column and washed with 10 × 10 mL of buffer A supplemented with 40 mM imidazole, and TioS(T₃) was eluted with 3 × 5 mL of buffer A supplemented with 500 mM imidazole. After SDS-PAGE analysis, the first two elution fractions that contained the protein of interest were dialyzed in 3 × 2 L of buffer B at 4 °C for a total of 20 h. The resulting solution was concentrated by using Amicon Ultra-15 Centrifugal Filter Units (EMD Millipore) with a 3 kDa MWCO membrane, and the concentration was spectrophotometrically determined by using the calculated extinction coefficient at 280 nm (<http://protcalc.sourceforge.net/cgi-bin/protcalc>). The yield of TioS(T₃) was 4.29 mg/L of culture (Figure S6).

Characterization of TioS(T₃) Activity by Trichloroacetic Acid (TCA) Precipitation Assays. To characterize the activity of TioS(T₃), conversion of the protein from its apo (inactive) to holo (active) form was monitored in the presence of Sfp (phosphopantetheinyltransferase) and [³H]AcCoA. Incorporation of [³H]acetyl into the TioS(T₃) apo-protein over time was assessed by using a TCA precipitation assay at room temperature as previously described.¹³ The total 25 μL reaction [75 mM Tris-HCl, 10 mM MgCl₂, 1 mM TCEP, 100 μM AcCoA containing ~160000 cpm of [³H]AcCoA, and 25 μM apo TioS(T₃), at pH 7.5] was initiated by addition of Sfp (1 μM). The reaction was quenched by adding 100 μL of a 10% TCA solution at 0, 2, 5, 10, and 30 min. The precipitate was pelleted by centrifugation at 14000 rpm for 7 min and washed twice with 100 μL of a 10% TCA solution. After the final wash, the pellets were dissolved in 100 μL of 88% formic acid. This was transferred into liquid scintillation vials containing 5 mL of the scintillation fluid, and the radiation activity was measured with a liquid scintillation counter (Figure S7).

To verify loading of L-Cys or N- or S-Me-L-Cys onto holo TioS(T₃), the apo to holo conversion was first performed for TioS(T₃) in a 12.5 μL reaction mixture (mixture A) for 30 min as described above, but by using CoA instead of [³H]AcCoA. Simultaneously, the activation of L-Cys to L-Cys-AMP was performed in a separate 12.5 μL reaction (mixture B) [75 mM Tris-HCl, 10 mM MgCl₂, 1 mM TCEP, 5 mM ATP, 5 μM TioS(A_{3a}M_{3s}A_{3b}) or TioN(A_aM_NA_b), and 1 mM L-Cys containing ~3500000 cpm of [³⁵S]L-Cys per reaction, at pH 7.5]. After substrate activation for 2 h, final concentrations of 5 μM for A domain and 5 mM for SAM or the same volume of H₂O was added to reaction mixture B, and the mixture was incubated for an additional 2 h. The loading reaction was initiated by combining reaction mixtures A and B and quenched by adding 100 μL of a 10% TCA solution at 0, 2, 5, 10, 30, 60, and 120 min. This was processed by the same method as described above (Figure 4). To precisely evaluate the loading of L-Cys in the presence and absence of SAM, the radioactivity of the reactions with different concentrations of TioS(T₃) was measured to draw V versus [TioS(T₃)] plots. The assay was performed under the same condition as described above, except

for various concentrations of TioS(T₃) (0, 25, 50, and 90 μM of the final concentration) and the radioactivity of [³⁵S]-L-Cys (~400000 cpm). The reaction was quenched at 120 min and the mixture processed by the same method as described above (Figure 4C).

Characterization of the Methyltransferase (M) Domain Activity of TioS(A_{3a}M₃₅A_{3b}) and TioN(A_aM_NA_b) by TCA Precipitation Assays. To evaluate the M domain activity of TioS(A_{3a}M₃₅A_{3b}) and TioN(A_aM_NA_b), time course TCA precipitation assays were performed by using L-Cys, N-Me-L-Cys, and S-Me-L-Cys as substrates. The time course was started after two sets of preincubation of reaction mixtures. The first reaction mixture, mixture A, which was prepared for adenylation of the substrate (L-Cys, N-Me-L-Cys, or S-Me-L-Cys), contained 10 μL of a solution comprised of 93.75 mM Tris-HCl, 12.5 mM MgCl₂, 1.25 mM TCEP, 3.125 mM ATP, 3.125 mM substrate, and 2.5 μM A domain, at pH 7.5. This was incubated for 2 h for L-Cys, 4 h for N-Me-L-Cys, and 6 h for S-Me-L-Cys. The second reaction mixture, mixture B, which was prepared for apo to holo conversion of TioS(T₃), contained 10 μL of a solution comprised of 93.75 mM Tris-HCl, 12.5 mM MgCl₂, 1.25 mM TCEP, 0.625 mM CoA, 125 μM TioS(T₃), and 1.25 μM Sfp, at pH 7.5. Mixture B was incubated for 30 min before being mixed with mixture A to create reaction mixture C for the loading of the activated substrate onto holo TioS(T₃). Reaction mixture C was further incubated for 4 h after the addition of extra A domain to maintain a concentration of 2.5 μM in this solution. Five microliters of a solution containing radioactive SAM (0.5 mM final concentration as in 25 μL with >3500000 cpm of [³H]SAM) was added to reaction mixture C to start the methylation process. This reaction was quenched at 0, 5, 10, 20, 30, 45, and 60 min by adding 100 μL of a 10% TCA solution and the mixture processed by the same method as described above in Characterization of TioS(T₃) Activity by Trichloroacetic Acid (TCA) Precipitation Assays (Figure 5).

To verify N-methylation at the secondary position of nitrogen on L-Cys by TioS(A_{3a}M₃₅A_{3b}), the following methylation assay was performed. N,S-DiMe-L-Cys was at first activated by TioN(A_aM_NA_b) in 6.25 μL of reaction mixture D [150 mM Tris-HCl, 20 mM MgCl₂, 2 mM TCEP, 4 mM ATP, 4 mM N,S-diMe-L-Cys, and 8 μM TioN(A_aM_NA_b), at pH 7.5], which was incubated overnight at room temperature. To prepare holo TioS(T₃), 11.25 μL of reaction mixture E [83.3 mM Tris, 11.1 mM MgCl₂, 1.1 mM TCEP, 556 μM CoA, 1.1 μM Sfp, and 192.2 μM TioS(T₃), at pH 7.5] was incubated for 15 min at room temperature. Reaction mixtures D and E were mixed together to create reaction mixture F before the addition of another portion of TioN(A_aM_NA_b) (50 μM in 1 μL; final concentration of 8 μM) and incubation for 5 h at room temperature. SAM (12.5 mM in 1 μL; final concentration of 676 μM) was added in mixture F to diminish the level of background methylation and incubated for an additional 4 h at room temperature. During the last 9 h of incubation, small amounts of TioN(A_aM_NA_b) were added every hour to achieve a final concentration of 10 μM in the final reaction mixture. [³H]SAM (1.5 μL, 900000 cpm) was added to reaction mixture F followed by addition of 5 μL of 50 μM TioS(A_{3a}M₃₅A_{3b}) or TioN(A_aM_NA_b) (as a negative control) to start the reaction, for a mixture that finally contained 75 mM Tris, 10 mM MgCl₂, 1 mM TCEP, 1 mM ATP, 1 mM N,S-diMe-L-Cys, 250 μM CoA, 0.5 μM Sfp, 500 μM SAM (with 900000 cpm of [³H]SAM), 86.5 μM TioS(T₃), 10 μM TioN(A_aM_NA_b), and 10 μM

TioS(A_{3a}M₃₅A_{3b}) or additional TioN(A_aM_NA_b). The reaction was quenched at 0, 1, 2, 4, 8, 16, 24, and 36 h by addition of 100 μL of a 10% TCA solution, and the mixture was processed by the same method as described above in Characterization of TioS(T₃) Activity by Trichloroacetic Acid (TCA) Precipitation Assays (Figure 6).

RESULTS AND DISCUSSION

Cloning, Heterologous (Co)expression, and Purification of Enzymes Used in This Study. To evaluate the proposed N- and S-methylating activity of TioS(A_{3a}M₃₅A_{3b}T₃) and TioN(A_aM_NA_b), respectively, and to determine if methylation occurs pre- or post-adenylation or pre- or post-thiolation, we separately cloned, overexpressed, and purified TioS(A_{3a}M₃₅A_{3b}) and TioS(T₃) (Figures S2 and S6). We also purified TioN(A_aM_NA_b) as we previously described.¹³ It has previously been shown that some A domains require an MbtH-like protein partner, which binds to the A domain around its a6 and a7 region,^{34–36} for their soluble expression,^{12,20,37–39} activity,^{40–43} and/or substrate specificity.⁴⁴ The two A domains involved in thiocoraline and thiochondrilline A studied so far [TioK(AT) and TioN(A_aM_NA_b)] required the MbtH-like protein partner TioT for their activity and/or soluble expression.^{13,20} We found that TioS(A_{3a}M₃₅A_{3b}) was not an exception to this observation and that it, too, could be expressed in a soluble and active form only when co-expressed with TioT (Figure S2).

Substrate Profile and Kinetic Characterization of the A Domains of TioS(A_{3a}M₃₅A_{3b}) and TioN(A_aM_NA_b). To assess if L-Cys is methylated [irrespective of the position (N or S)] before or after being adenylated (Figure 2, pathways a–c and g–i vs d–f and j–l), we first determined the substrate specificity of TioS(A_{3a}M₃₅A_{3b}) by an ATP–[³²P]PP_i exchange assay by surveying 20 natural L-amino acids, three methylated L-Cys derivatives (N-Me-, S-Me-, and N,S-diMe-L-Cys), and two additional L-Cys analogues [2-mercaptomethylbutyric acid (MMB) and 3-mercaptopyruvic acid (MP)] (Figure 3A). We

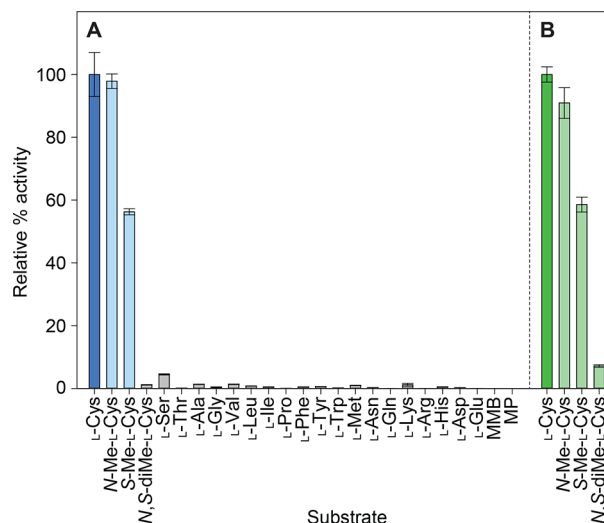


Figure 3. Relative substrate specificity of the A domain portion of (A) TioS(A_{3a}M₃₅A_{3b}) and (B) TioN(A_aM_NA_b) co-expressed with TioT (2.5 μM), as determined by ATP–[³²P]PP_i exchange assays at a 2 h end point. The substrates for which kinetic parameters were determined (Table 1) are designated by the dark or light blue or green bars.

found that L-Cys was the best substrate for TioS(A_{3a}M₃₅A_{3b}) and that N-Me-L-Cys and S-Me-L-Cys could also be activated at 98 and 56%, respectively, when compared to L-Cys. However, N,S-diMe-L-Cys was not activated at all by TioS(A_{3a}M₃₅A_{3b}). These data show that N,S-dimethylation cannot happen prior to adenylation by TioS(A_{3a}M₃₅A_{3b}) and thereby exclude pathways a and g. To test if L-Cys was the natural substrate for TioS(A_{3a}M₃₅A_{3b}), we determined Michaelis–Menten kinetic parameters for each substrate (Table 1 and Figure S3). Although the maximum turnover rates (k_{cat}) were not significantly different among the three substrates tested, their affinities for this enzyme varied significantly, with the K_m of L-Cys being the smallest, followed by that of N-Me-L-Cys (15-fold higher than that of L-Cys) and then that of S-Me-L-Cys (70-fold higher than that of L-Cys). The overall catalytic efficiency (k_{cat}/K_m) for L-Cys was 14- and 84-fold higher than those for N-Me-L-Cys and S-Me-L-Cys, respectively. These kinetic data strongly suggest that neither N- nor S-methylation occurs prior to adenylation, excluding pathways b, c, h, and i in addition to pathways a and g that have been eliminated by the substrate profile assay. These TioS(A_{3a}M₃₅A_{3b}) results are also consistent with our previous preliminary report showing that methylation of L-Cys by TioN occurs post-adenylation, providing a convincing answer (to question ia) that methylation post-adenylation is favored over methylation pre-adenylation.¹³

Although a substrate profile of TioN(A_aM_NA_b) was already reported,¹³ it did not include N-Me-L-Cys or N,S-diMe-L-Cys. Therefore, we performed ATP–[³²P]PP_i exchange assays to assess the substrate profile and kinetic parameters of TioN(A_aM_NA_b) for L-Cys and its methylated derivatives (Figure 3B, Table 1, and Figure S4). Even though L-Cys and S-Me-L-Cys had been previously tested,¹³ we used them again in this study to ensure self-consistent experiments with the newly purified TioN(A_aM_NA_b) enzyme. Both the substrate profile and kinetic parameters for TioN(A_aM_NA_b) showed trends similar to those observed with TioS(A_{3a}M₃₅A_{3b}). L-Cys remained the substrate of choice for TioN(A_aM_NA_b), followed by N-Me-L-Cys and S-Me-L-Cys, which were activated at 91 and 59%, respectively, when compared to L-Cys. Interestingly, while adenylation of N,S-diMe-L-Cys was basically undetectable with TioS(A_{3a}M₃₅A_{3b}), adenylation of this compound by TioN(A_aM_NA_b) could be observed (7% activity compared to L-Cys). Like what was observed with TioS(A_{3a}M₃₅A_{3b}), the rank order of catalytic efficiencies of TioN(A_aM_NA_b) with L-Cys and its methylated derivatives (22- and 104-fold lower for N-Me-L-Cys and S-Me-L-Cys, respectively, than for L-Cys) was determined by the affinity of these substrates (29- and 95-fold higher for N-Me-L-Cys and S-Me-L-Cys, respectively, than for L-Cys) for the enzyme and did not heavily rely on the k_{cat} values. Although N,S-diMe-L-Cys was found to be a poor substrate of TioN(A_aM_NA_b), the steady-state kinetic parameters for its AMP derivatization could not be determined as the enzyme function was inhibited by a high concentration of the substrate (>5 mM), where the plot of V_{max} versus [N,S-diMe-L-Cys] remains linear (Figure S5). Overall, these series of ATP–[³²P]PP_i exchange assays with TioS(A_{3a}M₃₅A_{3b}) and TioN(A_aM_NA_b) unequivocally narrow down the possible pathway for the preparation of N,S-diMe-L-Cys-S-TioS(T₃) to one in which L-Cys is first converted to L-Cys-AMP by the A domain of TioS(A_{3a}M₃₅A_{3b}) (Figure 2, pathways d–f and j–l).

Assay of Loading of [³⁵S]-L-Cys onto TioS(T₃) in the Presence or Absence of SAM. We next tested if loading of L-Cys onto TioS(T₃) was affected by SAM, which could indicate

whether methylation occurred pre- or post-thiolation (our question ib). We compared the loading onto TioS(T₃) of the activated [³⁵S]-L-Cys (Figure 2, step f₂ or l₂), N-Me-[³⁵S]-L-Cys produced by TioS(A_{3a}M₃₅A_{3b}) (Figure 2, step k₃), and S-Me-[³⁵S]-L-Cys generated by TioN(A_aM_NA_b) (Figure 2, step e₃) in a TCA precipitation time course assay using [³⁵S]-L-Cys as the starting point in the absence and presence of SAM (Figure 4A,B). In this assay, TioS(T₃) was at first posttranslationally modified by a PPTase and CoA. T domains of NRPSs are expressed in their apo form, and a PPTase is necessary to

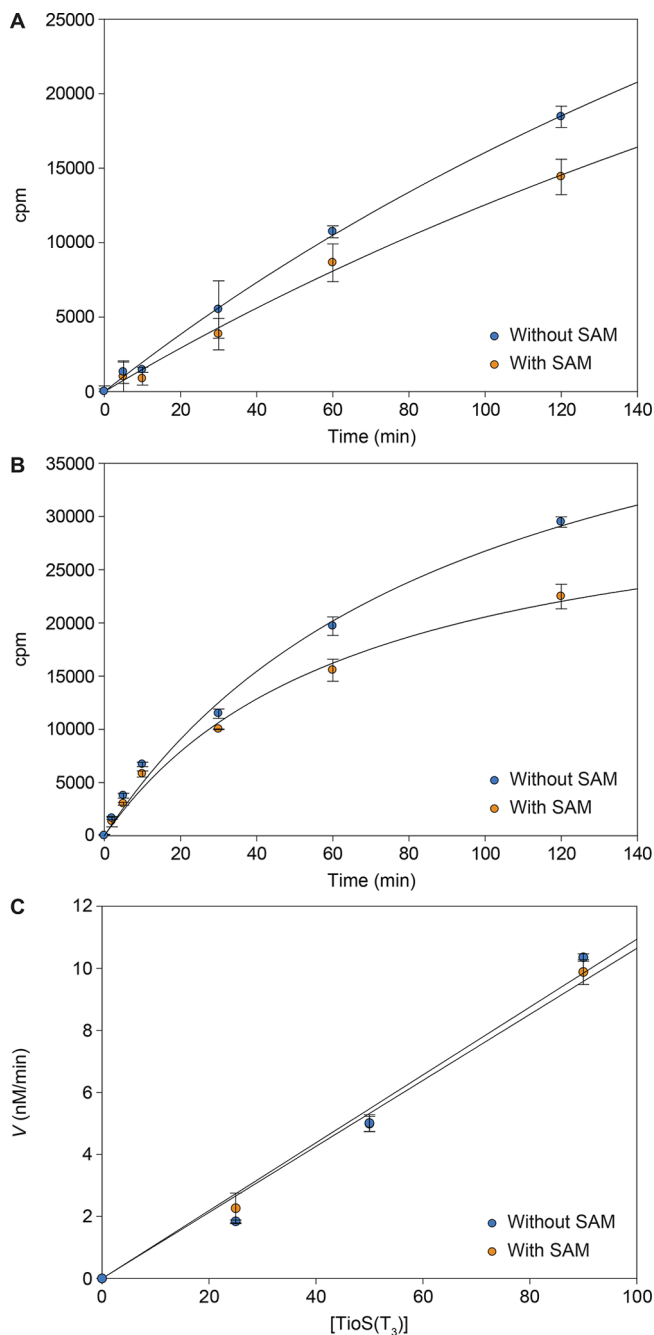


Figure 4. (A and B) Time courses and (C) TioS(T₃) concentration-dependent velocity to monitor the loading of [³⁵S]-L-Cys-AMP onto TioS(T₃) in the absence (blue circles) or presence (orange circles) of SAM by TCA precipitation assays. [³⁵S]-L-Cys was activated and loaded onto TioS(T₃) by using TioS(A_{3a}M₃₅A_{3b}) (A and C) or TioN(A_aM_NA_b) (B).

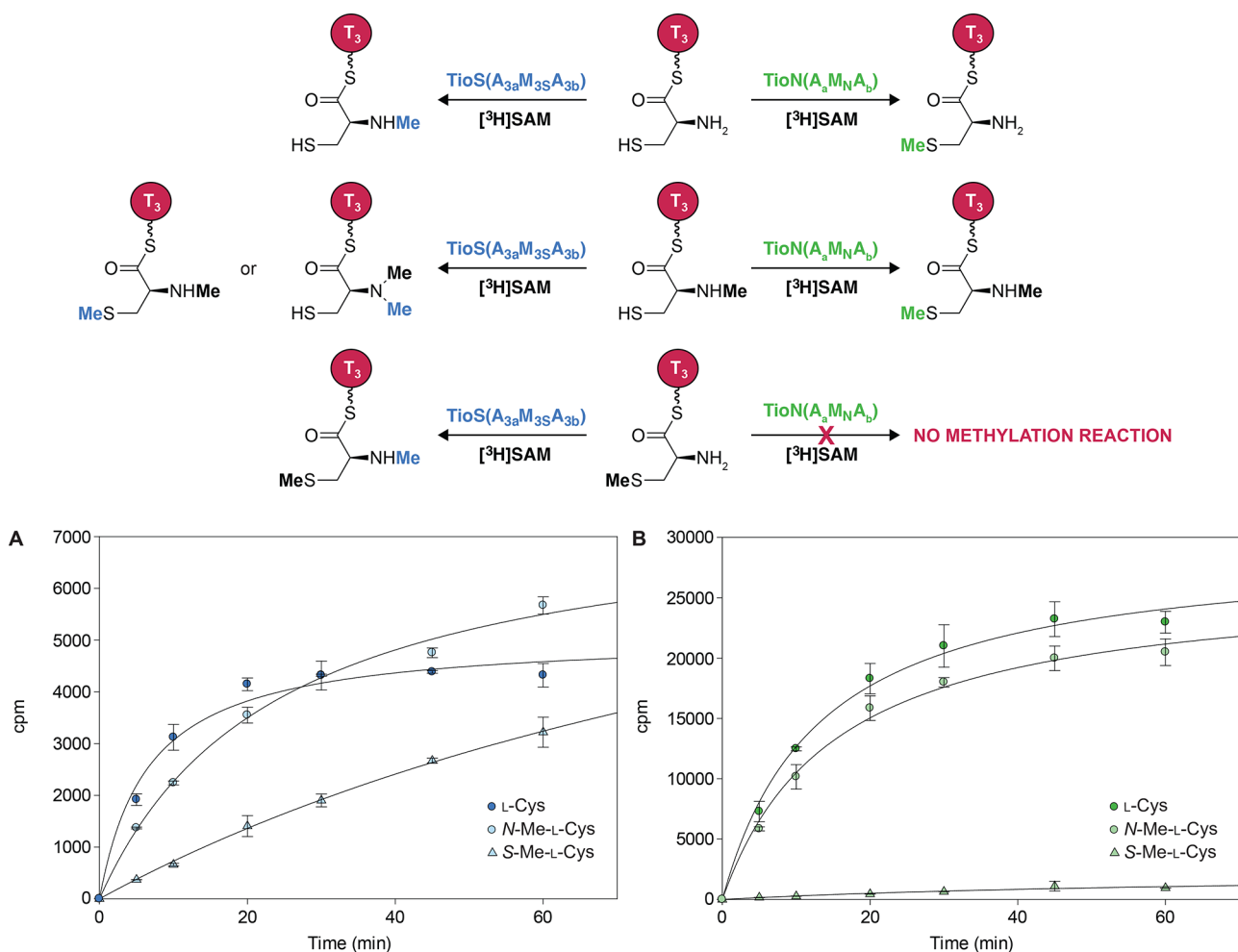


Figure 5. Methylation of L-Cys-S-TioS(T_3), N-methyl-L-Cys-S-TioS(T_3), and S-methyl-L-Cys-S-TioS(T_3) by (A) TioS($A_{3a}M_{3S}A_{3b}$) or (B) TioN($A_aM_NA_b$) with [3H]SAM as a methylating agent, measured by TCA precipitation assays.

transfer the flexible Ppant arm from CoA to a conserved serine residue of T domains to render them holo. We showed that TioS(T_3) could be converted from its apo to holo form by a TCA precipitation assay using [3H]acetyl-CoA and the well-known promiscuous PPTase Sfp²⁹ (Figure S7). The separately activated holo TioS(T_3) was mixed with a reaction solution in which SAM (or H $_2$ O as a control) was added after adenylation of the [^{35}S]-L-Cys substrate by either TioS($A_{3a}M_{3S}A_{3b}$) or TioN($A_aM_NA_b$) (Figure 4). We measured the radioactivity of the loaded TioS(T_3) in time courses for both enzymes (Figure 4A,B) or at 120 min for TioS($A_{3a}M_{3S}A_{3b}$) with different concentrations of the T domain to calculate the velocity of the loading activity at each TioS(T_3) concentration (Figure 4C). We observed that [^{35}S]-L-Cys was loaded onto TioS(T_3) with similar efficiencies in the presence and absence of SAM. This experiment suggests that the loading step is fast and likely proceeds with L-Cys-AMP prior to its methylation (which cannot be observed directly in this experiment). These data indicate that pathways f and l are favored over pathways d, e, j, and k. This order is consistent with the recent crystal structure of the adenylation–formylation–thiolation tridomain, where the thiolation domain loads the amino acid residue (by using the adenylation residue as a substrate) prior to its formylation.⁴⁵

Methylation Assay of L-Cys, N-Me-L-Cys, and S-Me-L-Cys with [3H]SAM. Having narrowed down the biosynthesis of N,S-diMe-L-Cys-S-TioS(T_3) from 12 to two possible

pathways (f and l), we next focused on determining if L-Cys could be sequentially dimethylated by two independent interrupted A domains (our question iia,b). To assess if methylation of L-Cys-S-TioS(T_3) first happens on the nitrogen of the L-Cys backbone (Figure 2, step l₃) or on the sulfur of its side chain (Figure 2, step f₃), methylation of L-Cys-S-TioS(T_3), N-Me-L-Cys-S-TioS(T_3), and S-Me-L-Cys-S-TioS(T_3), which are the only possible M domain substrates remaining on the basis of the experiments described above, by TioS($A_{3a}M_{3S}A_{3b}$) or TioN($A_aM_NA_b$) was assessed by TCA precipitation assays using [3H]SAM (our question iib). After activation by the A domain portions of TioS($A_{3a}M_{3S}A_{3b}$) or TioN($A_aM_NA_b$), the substrate AMPs were loaded onto holo TioS(T_3). After loading for 4 h, when we assumed that TioS(T_3) was fully modified with the expected L-Cys, N-Me-L-Cys, or S-Me-L-Cys species, radioactive [3H]SAM was added to the reaction mixture to measure the methylating activity in time course assays (Figure 5). Not surprisingly, we found that both TioS($A_{3a}M_{3S}A_{3b}$) (Figure 5A) and TioN($A_aM_NA_b$) (Figure 5B) were capable of methylating their natural substrate L-Cys covalently attached to TioS(T_3) (Figure 5, top reactions). Also, as predicted, we observed that S-Me-L-Cys-S-TioS(T_3) was not a substrate for additional methylation by TioN($A_aM_NA_b$), confirming that this enzyme is an S-methyltransferase (Figure 5B and bottom right reaction). However, when it was reacted with TioS($A_{3a}M_{3S}A_{3b}$), we observed that S-Me-L-Cys-S-TioS(T_3) could be further N-

methylated, albeit not as effectively as L-Cys-S-TioS(T_3) (Figure 5A and bottom left reaction). Similarly, we found that N-Me-L-Cys-S-TioS(T_3) could be further S-methylated by TioN($A_aM_NA_b$), but in this case, the additional methylation proceeded as efficiently as that of L-Cys-S-TioS(T_3) (Figure 5B and middle right reaction). These data strongly suggest that TioS($A_{3a}M_{3S}A_{3b}$) and TioN($A_aM_NA_b$) can sequentially and specifically methylate the backbone and then the side chain of L-Cys while it is tethered to TioS(T_3), not only providing answers to our question iia,b, but also pointing to pathway I in Figure 2 as the favored sequence of events followed by Nature for the biosynthesis of N,S-diMe-L-Cys-S-TioS(T_3). Although this is only speculation (as there are currently no available structures of A domains interrupted by M domains), the fact that TioS($A_{3a}M_{3S}A_{3b}$) is physically connected to TioS(T_3) in the thiocoraline/thiochondrilline A gene cluster, while TioN is a stand-alone enzyme, could potentially explain two intriguing observations. The first is why the M domain of TioS($A_{3a}M_{3S}A_{3b}$), which should be closer in space and more available, could act first to N-methylate the L-Cys attached to TioS(T_3). The second is why the M domain of TioN($A_aM_NA_b$), which is in its naturally occurring form, has an activity higher than that of TioS($A_{3a}M_{3S}A_{3b}$), which likely has a relatively larger loss of activity because of its excision from the TioS protein.

While evaluating the ability of TioS($A_{3a}M_{3S}A_{3b}$) to further methylate N-Me-L-Cys-S-TioS(T_3), we made the unexpected and puzzling observation that this substrate could be further methylated by the enzyme (Figure 5A and middle left reaction). This observation could indicate that TioS($A_{3a}M_{3S}A_{3b}$) is capable either of both backbone and side-chain methylation to produce N,S-diMe-L-Cys-S-TioS(T_3) on its own or of dimethylation of the backbone to produce N,N-diMe-L-Cys-S-TioS(T_3); neither of these phenomena has ever been reported.

Methylation Assay of N,S-DiMe-L-Cys with [3 H]SAM. To solve the TioS($A_{3a}M_{3S}A_{3b}$) dimethylation puzzle described above, we utilized N,S-diMe-L-Cys-S-TioS(T_3) in time course methylation assays (Figure 6). We took advantage of the fact that N,S-diMe-L-Cys can be activated by TioN($A_aM_NA_b$) at a very slow rate (Figure S5) and loaded it onto TioS(T_3) to prepare the N,S-diMe-L-Cys-S-TioS(T_3) used in these methylation assays. Prior to studying the dimethylation by TioS($A_{3a}M_{3S}A_{3b}$), although we suspected that TioN($A_aM_NA_b$) would not interfere in the assay because we established that it does not N-methylate S-Me-L-Cys-S-TioS(T_3) (Figure 5B and bottom right reaction), we first confirmed that this was the case by concomitantly performing the assay with TioN($A_aM_NA_b$) and observing no activity (Figure 6, white circles). We then performed the methylation assay with TioS($A_{3a}M_{3S}A_{3b}$) and N,S-diMe-L-Cys-S-TioS(T_3) and found this substrate to be N-methylated (Figure 6, blue circles). These results clearly show that the second methylation performed by TioS($A_{3a}M_{3S}A_{3b}$), which we observed in Figure 5, occurs on the backbone of the amino acid and not on the sulfur atom of its side chain.

CONCLUSION

In summary, this study revealed that (i) adenylation happens prior to methylations, which themselves likely occur only after loading of the activated amino acids onto T domains, (ii) two interrupted A domains can work sequentially to methylate first the backbone and then the side chain of a single amino acid,

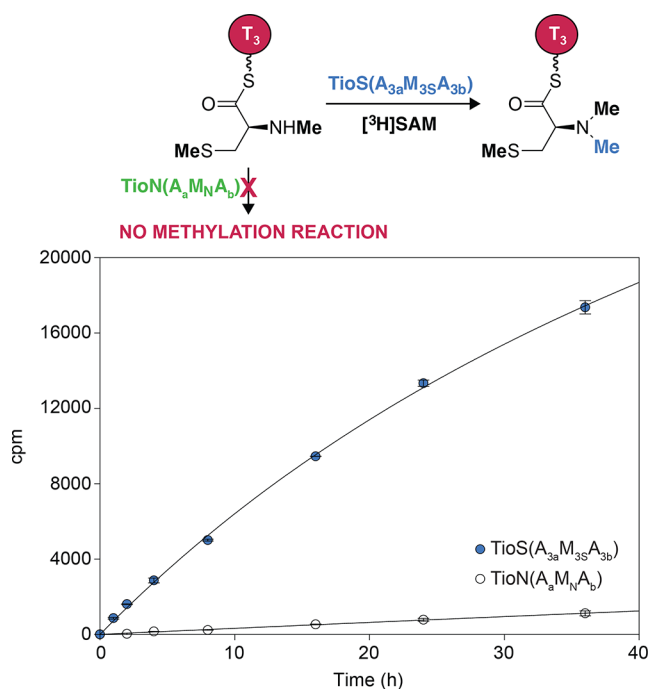


Figure 6. Methylation of N,S-dimethyl-L-Cys-S-TioS(T_3) by TioS($A_{3a}M_{3S}A_{3b}$) (blue circles) or TioN($A_aM_NA_b$) (white circles, as a negative control) with [3 H]SAM as a methylating agent, measured by TCA precipitation assays.

and (iii) one interrupted A domain is not capable of methylating both the backbone and side chain of a given amino acid residue. However, we serendipitously discovered that A domains interrupted between their a8 and a9 motifs by M domains can perform amino acid backbone dimethylation. This work provides a deeper understanding of how bifunctional A/M domains function and lays the foundation for future engineering of unique bi- and trifunctional interrupted A domains to serve in the development of novel biologically active natural product-derived compounds. Such work is currently underway in our laboratory.

ASSOCIATED CONTENT

Supporting Information

The Supporting Information is available free of charge on the ACS Publications website at DOI: 10.1021/acs.biochem.7b00980.

A table of primers used to clone the various constructs for protein overexpression (Table S1), synthetic schemes used for potential substrate synthesis (Figure S1), SDS-PAGE gels for TioS($A_{3a}M_{3S}A_{3b}$) (Figure S2) and TioS(T_3) (Figure S6), Michaelis–Menten plots for TioS($A_{3a}M_{3S}A_{3b}$) (Figure S3) and TioN($A_aM_NA_b$) (Figure S4), the time course for adenylation of N,S-diMe-L-Cys by TioN($A_aM_NA_b$) (Figure S5), and the apo to holo conversion of TioS(T_3) (Figure S7) (PDF)

AUTHOR INFORMATION

Corresponding Author

*E-mail: sylviegt@sodikova@uky.edu.

ORCID

Sylvie Garneau-Tsodikova: 0000-0002-7961-5555

Author Contributions

S.M. and S.G.-T. designed the study. S.M., O.V.T., and S.G.-T. analyzed the data and wrote the manuscript. S.M. performed all biochemical experiments. A.G. performed chemical synthesis.

Funding

This project was supported by National Science Foundation CAREER Award MCB-1149427 (to S.G.-T.) and by start-up funds from the College of Pharmacy at the University of Kentucky (to S.G.-T.).

Notes

The authors declare no competing financial interest.

REFERENCES

- (1) Newman, D. J., and Cragg, G. M. (2016) Natural products as sources of new drugs from 1981 to 2014. *J. Nat. Prod.* 79, 629–661.
- (2) Weissman, K. J. (2015) The structural biology of biosynthetic megaenzymes. *Nat. Chem. Biol.* 11, 660–670.
- (3) Fischbach, M. A., and Walsh, C. T. (2006) Assembly-line enzymology for polyketide and nonribosomal peptide antibiotics: logic, machinery, and mechanisms. *Chem. Rev.* 106, 3468–3496.
- (4) Walsh, C. T. (2016) Insights into the chemical logic and enzymatic machinery of NRPS assembly lines. *Nat. Prod. Rep.* 33, 127–135.
- (5) Park, H. B., Kim, Y. J., Park, J. S., Yang, H. O., Lee, K. R., and Kwon, H. C. (2011) Glionitrin B, a cancer invasion inhibitory diketopiperazine produced by microbial coculture. *J. Nat. Prod.* 74, 2309–2312.
- (6) Bhuiya, M. W., and Liu, C. J. (2010) Engineering monoglucosyl-O-methyltransferases to modulate lignin biosynthesis. *J. Biol. Chem.* 285, 277–285.
- (7) Zhang, Q., and van der Donk, W. A. (2012) Catalytic promiscuity of a bacterial alpha-N-methyltransferase. *FEBS Lett.* 586, 3391–3397.
- (8) Itoh, N., Iwata, C., and Toda, H. (2016) Molecular cloning and characterization of a flavonoid-O-methyltransferase with broad substrate specificity and regioselectivity from *Citrus depressa*. *BMC Plant Biol.* 16, 180.
- (9) Kim, E., Song, M. C., Kim, M. S., Beom, J. Y., Lee, E. Y., Kim, D. M., Nam, S. J., and Yoon, Y. J. (2016) Characterization of the two methylation steps involved in the biosynthesis of mycinose in tylosin. *J. Nat. Prod.* 79, 2014–2021.
- (10) Singh, S., Zhang, J., Huber, T. D., Sunkara, M., Hurley, K., Goff, R. D., Wang, G., Zhang, W., Liu, C., Rohr, J., Van Lanen, S. G., Morris, A. J., and Thorson, J. S. (2014) Facile chemoenzymatic strategies for the synthesis and utilization of S-adenosyl-(L)-methionine analogues. *Angew. Chem., Int. Ed.* 53, 3965–3969.
- (11) Labby, K. J., Watsula, S. G., and Garneau-Tsodikova, S. (2015) Interrupted adenylation domains: unique bifunctional enzymes involved in nonribosomal peptide biosynthesis. *Nat. Prod. Rep.* 32, 641–653.
- (12) Zolova, O. E., and Garneau-Tsodikova, S. (2014) KtzJ-dependent serine activation and O-methylation by KtzH for kutznerides biosynthesis. *J. Antibiot.* 67, 59–64.
- (13) Al-Mestarihi, A. H., Villamizar, G., Fernandez, J., Zolova, O. E., Lombó, F., and Garneau-Tsodikova, S. (2014) Adenylation and S-methylation of cysteine by the bifunctional enzyme TioN in thiocoraline biosynthesis. *J. Am. Chem. Soc.* 136, 17350–17354.
- (14) Shrestha, S. K., and Garneau-Tsodikova, S. (2016) Expanding substrate promiscuity by engineering a novel adenylation-methylating NRPS bifunctional enzyme. *ChemBioChem* 17, 1328–1332.
- (15) Schwarzer, D., Finking, R., and Marahiel, M. A. (2003) Nonribosomal peptides: from genes to products. *Nat. Prod. Rep.* 20, 275–287.
- (16) Conti, E., Stachelhaus, T., Marahiel, M. A., and Brick, P. (1997) Structural basis for the activation of phenylalanine in the non-ribosomal biosynthesis of gramicidin S. *EMBO J.* 16, 4174–4183.
- (17) Stachelhaus, T., Mootz, H. D., and Marahiel, M. A. (1999) The specificity-conferring code of adenylation domains in nonribosomal peptide synthetases. *Chem. Biol.* 6, 493–505.
- (18) Mady, A. S., Zolova, O. E., Millan, M. A., Villamizar, G., de la Calle, F., Lombó, F., and Garneau-Tsodikova, S. (2011) Characterization of TioQ, a type II thioesterase from the thiocoraline biosynthetic cluster. *Mol. Biosyst.* 7, 1999–2011.
- (19) Sheoran, A., King, A., Velasco, A., Pero, J. M., and Garneau-Tsodikova, S. (2008) Characterization of TioF, a tryptophan 2,3-dioxygenase involved in 3-hydroxyquinolindole acid formation during thiocoraline biosynthesis. *Mol. Biosyst.* 4, 622–628.
- (20) Zolova, O. E., and Garneau-Tsodikova, S. (2012) Importance of the MbtH-like protein TioT for production and activation of the thiocoraline adenylation domain of TioK. *MedChemComm* 3, 950–955.
- (21) Zolova, O. E., Mady, A. S., and Garneau-Tsodikova, S. (2010) Recent developments in bisintercalator natural products. *Biopolymers* 93, 777–790.
- (22) Biswas, T., Zolova, O. E., Lombó, F., de la Calle, F., Salas, J. A., Tsodikov, O. V., and Garneau-Tsodikova, S. (2010) A new scaffold of an old protein fold ensures binding to the bisintercalator thiocoraline. *J. Mol. Biol.* 397, 495–507.
- (23) Mori, S., Shrestha, S. K., Fernandez, J., Alvarez San Millan, M., Garzan, A., Al-Mestarihi, A. H., Lombó, F., and Garneau-Tsodikova, S. (2017) Activation and loading of the starter unit during thiocoraline biosynthesis. *Biochemistry* 56, 4457–4467.
- (24) McQuade, T. J., Shalloo, A. D., Sheoran, A., Delproposto, J. E., Tsodikov, O. V., and Garneau-Tsodikova, S. (2009) A nonradioactive high-throughput assay for screening and characterization of adenylation domains for nonribosomal peptide combinatorial biosynthesis. *Anal. Biochem.* 386, 244–250.
- (25) Garneau-Tsodikova, S., Dorrestein, P. C., Kelleher, N. L., and Walsh, C. T. (2006) Protein assembly line components in prodigiosin biosynthesis: characterization of PigA, G,H, I,J. *J. Am. Chem. Soc.* 128, 12600–12601.
- (26) Tsodikov, O. V., Hou, C., Walsh, C. T., and Garneau-Tsodikova, S. (2015) Crystal structure of O-methyltransferase CalO6 from the calicheamicin biosynthetic pathway: a case of challenging structure determination at low resolution. *BMC Struct. Biol.* 15, 13.
- (27) Perez Baz, J., Canedo, L. M., Fernandez Puentes, J. L., and Silva Elipe, M. V. (1997) Thiocoraline, a novel depsipeptide with antitumor activity produced by a marine *Micromonospora*. II. Physico-chemical properties and structure determination. *J. Antibiot.* 50, 738–741.
- (28) Wyche, T. P., Hou, Y., Braun, D., Cohen, H. C., Xiong, M. P., and Bugni, T. S. (2011) First natural analogs of the cytotoxic thiodepsipeptide thiocoraline A from a marine *Verrucospora* sp. *J. Org. Chem.* 76, 6542–6547.
- (29) Quadri, L. E., Weinreb, P. H., Lei, M., Nakano, M. M., Zuber, P., and Walsh, C. T. (1998) Characterization of Sfp, a *Bacillus subtilis* phosphopantetheinyl transferase for peptidyl carrier protein domains in peptide synthetases. *Biochemistry* 37, 1585–1595.
- (30) Liu, J.-F., Tang, X.-X., and Jiang, B. (2002) A convenient synthesis of N-fluorenylmethoxycarbonyl-N-methyl-L-cysteine derivatives [Fmoc,Me-Cys(R)-OH]. *Synthesis* 11, 1499–1501.
- (31) Nudelman, A., Marcovici-Mizrahi, D., Nudelman, A., Flint, D., and Wittenbach, V. (2004) Inhibitors of biotin biosynthesis as potential herbicides. *Tetrahedron* 60, 1731–1748.
- (32) Lee, H. S., and Kim, D. H. (2003) Synthesis and evaluation of alpha,alpha-disubstituted-3-mercaptopropanoic acids as inhibitors for carboxypeptidase A and implications with respect to enzyme inhibitor design. *Bioorg. Med. Chem.* 11, 4685–4691.
- (33) de Castro, M. V., Ioca, L. P., Williams, D. E., Costa, B. Z., Mizuno, C. M., Santos, M. F., de Jesus, K., Ferreira, E. L., Selegim, M. H., Sette, L. D., Pereira Filho, E. R., Ferreira, A. G., Goncalves, N. S., Santos, R. A., Patrick, B. O., Andersen, R. J., and Berlinck, R. G. (2016) Condensation of macrocyclic polyketides produced by *Penicillium* sp. DRF2 with mercaptopyruvate represents a new fungal detoxification pathway. *J. Nat. Prod.* 79, 1668–1678.

(34) Herbst, D. A., Boll, B., Zocher, G., Stehle, T., and Heide, L. (2013) Structural basis of the interaction of MbtH-like proteins, putative regulators of nonribosomal peptide biosynthesis, with adenylation enzymes. *J. Biol. Chem.* 288, 1991–2003.

(35) Miller, B. R., Drake, E. J., Shi, C., Aldrich, C. C., and Gulick, A. M. (2016) Structures of a nonribosomal peptide synthetase module bound to MbtH-like proteins support a highly dynamic domain architecture. *J. Biol. Chem.* 291, 22559–22571.

(36) Tarry, M. J., Haque, A. S., Bui, K. H., and Schmeing, T. M. (2017) X-Ray crystallography and electron microscopy of cross- and multi-module nonribosomal peptide synthetase proteins reveal a flexible architecture. *Structure* 25, 783–793.

(37) Heemstra, J. R., Jr., Walsh, C. T., and Sattely, E. S. (2009) Enzymatic tailoring of ornithine in the biosynthesis of the *Rhizobium* cyclic trihydroxamate siderophore vicibactin. *J. Am. Chem. Soc.* 131, 15317–15329.

(38) Imker, H. J., Krahn, D., Clerc, J., Kaiser, M., and Walsh, C. T. (2010) *N*-acylation during glidobactin biosynthesis by the tridomain nonribosomal peptide synthetase module GlbF. *Chem. Biol.* 17, 1077–1083.

(39) McMahon, M. D., Rush, J. S., and Thomas, M. G. (2012) Analyses of MbtB, MbtE, and MbtF suggest revisions to the mycobactin biosynthesis pathway in *Mycobacterium tuberculosis*. *J. Bacteriol.* 194, 2809–2818.

(40) Boll, B., Taubitz, T., and Heide, L. (2011) Role of MbtH-like proteins in the adenylation of tyrosine during aminocoumarin and vancomycin biosynthesis. *J. Biol. Chem.* 286, 36281–36290.

(41) Zhang, C., Kong, L., Liu, Q., Lei, X., Zhu, T., Yin, J., Lin, B., Deng, Z., and You, D. (2013) *In vitro* characterization of echinomycin biosynthesis: formation and hydroxylation of l-tryptophanyl-S-enzyme and oxidation of (2*S*,3*S*) beta-hydroxytryptophan. *PLoS One* 8, e56772.

(42) Zhang, W., Heemstra, J. R., Jr., Walsh, C. T., and Imker, H. J. (2010) Activation of the pacidamycin PacL adenylation domain by MbtH-like proteins. *Biochemistry* 49, 9946–9947.

(43) Felnagle, E. A., Barkei, J. J., Park, H., Podevels, A. M., McMahon, M. D., Drott, D. W., and Thomas, M. G. (2010) MbtH-like proteins as integral components of bacterial nonribosomal peptide synthetases. *Biochemistry* 49, 8815–8817.

(44) Davidsen, J. M., Bartley, D. M., and Townsend, C. A. (2013) Nonribosomal propeptide precursor in nocardicin A biosynthesis predicted from adenylation domain specificity dependent on the MbtH family protein NoC1. *J. Am. Chem. Soc.* 135, 1749–1759.

(45) Reimer, J. M., Aloise, M. N., Harrison, P. M., and Schmeing, T. M. (2016) Synthetic cycle of the initiation module of a formylating nonribosomal peptide synthetase. *Nature* 529, 239–242.